Stanford Exploration Project, Report 79, November 16, 1997, pages 73–82

Stanford Exploration Project, Report 79, November 16, 1997, pages 73–82

Toward estimating near surface lateral velocity variations

Dimitri Bevc[1]

keywords: *velocity, near surface, slant stack, anomaly*

ABSTRACT

Near surface velocity irregularities distort the seismic wavefield and cause focusing anomalies in the data. These anomalies can be detected by examining plots of trace power in midpoint-offset coordinates.
I generate synthetic data by upward continuing a synthetic wavefield through a $v(x, z)$ model. The location of the velocity anomaly is determined by analyzing a plot of trace power in midpoint-offset coordinates. By performing iterative slant stacks of the power plots, I can image the velocity anomaly. Finally, I downward continue the wavefield through the velocity anomaly in order to remove distortions from the data.

INTRODUCTION

The near surface presents many problems for seismologists, but it should also present many opportunities. While there are often severe velocity and absorption anomalies in the near surface, the recorded wavefield samples this region densely. Kjartansson (Kjartansson, 1979; Claerbout, 1985) developed a method of locating lateral velocity variations. His method is based on taking the trace power in some time window and performing slant stacks of the power maps in order to determine the anomaly depth. The idea is that energy aligned along the midpoint axis is due to anomalies at depth and energy aligned closer to the shot and geophone axes is due to shallow anomalies. Claerbout (1993) repeats Kjartansson work and proposes a method of performing reflection tomography without picking.

I outline a method which incorporates Kjartansson's (1979) method and wavefield extrapolation to estimate near surface velocity distribution. The methodology is not yet complete, but the building blocks are being put in place. It is these building blocks that I present in this report.

I begin by modeling shallow velocity anomalies which are shorter in lateral ex-

[1]**email:** not available

tent than the spread length. Synthetic data are generated by upward continuing a synthetic wavefield through a $v(x,z)$ model. The location of the velocity anomaly is determined by analyzing a plot of trace power in midpoint-offset coordinates. The trace power plots are then input to an iterative slant-stack algorithm to generate images of the velocity anomalies. I downward continue the data through the $v(x,z)$ model to demonstrate that distortions due to the anomaly can be removed. This method can be used as an iterative inversion process to determine near surface velocity.

MODELING NEAR SURFACE LATERAL VELOCITY VARIATION

The velocity model used for this study consists of two reflectors and a near surface velocity perturbation (Figure 1). The velocity perturbation consists of a low velocity zone bounded by two Gaussian shaped surfaces.

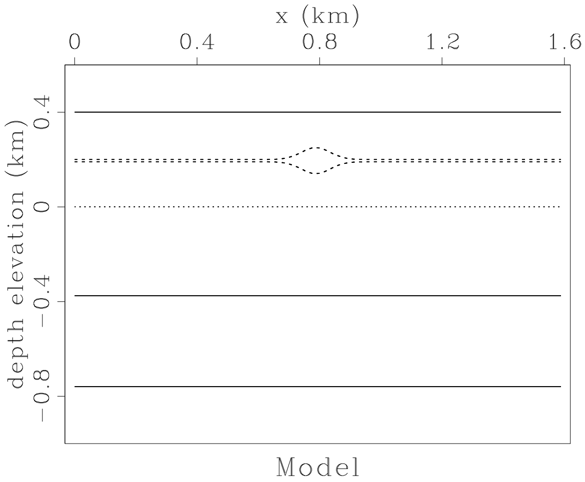

Figure 1: Two horizontal reflectors at $-0.4\ km$ and $-0.8\ km$ are represented by solid lines. Synthetic data are initially generated at the surface represented by the dotted line. This data is then upward continued through the two surfaces represented by the dashed lines up to the solid line at $0.4\ km$. The medium velocity is $2\ km/s$ everywhere except between the two dashed lines where it is $1.5\ km/s$. dimitri-model [ER]

Synthetic data are generated using two Kirchhoff modeling programs. I first generate constant velocity synthetic shot gathers (Figure 2a) using a constant offset migration and modeling program similar to the program described in a previous report (Bevc and Claerbout, 1993). These synthetic gathers are generated at a depth of $0\ km$ (Figure 1). The synthetic data are then upward continued to an elevation of $0.4\ km$ using a data parallel Kirchhoff datuming algorithm (Bevc, 1993). The upward continuation is performed in three steps, using constant velocities in each step. The first upward continuation transforms the data from the flat surface at $0\ km$ to the Gaussian surface $0.19\ km$. The data are then upward continued with a low velocity to the next Gaussian surface. The complete synthetic data set is generated by upward continuing the data to the level surface at elevation $0.4\ km$.

The effect of the low velocity perturbation can be seen in Figure 2b as a timing and focusing anomaly. Because of the focusing effect, a static shift of the data is not adequate to correct for the velocity perturbation. As the shot number increases, the anomaly moves from right to left across the gathers. There are some artifacts in the synthetics because of data truncation effects and the rapid undulation of the Gaussian boundary.

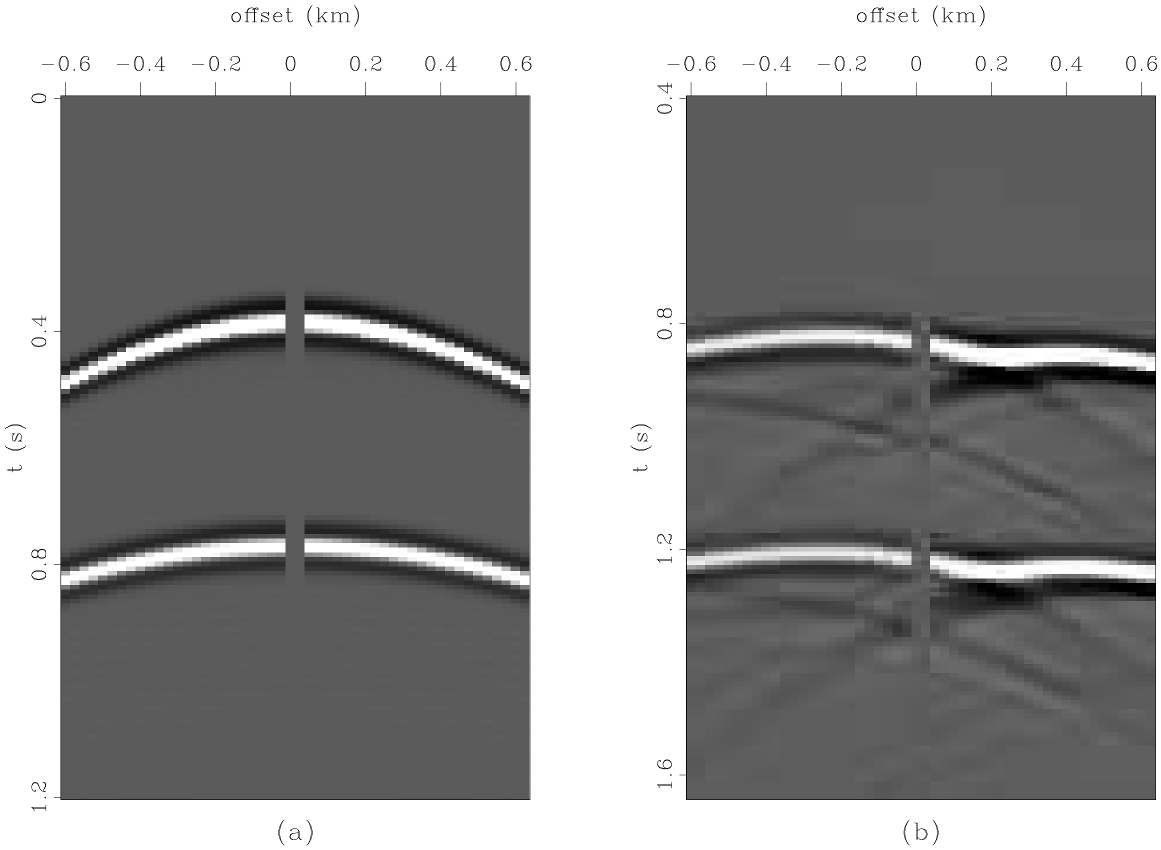

Figure 2: A synthetic shot gather (a) before upward continuation and (b) after upward continuation through the near surface velocity anomaly. The effect of the velocity perturbation is to cause a timing shift and a focusing anomaly in the synthetic data. dimitri-shot [ER]

NEAR SURFACE VELOCITY ANOMALIES OBSERVED

The synthetic data are sorted into common midpoint gathers and NMO corrected. The resulting data cube is displayed in Figure 3. The effect of the velocity anomaly is seen as a symmetric "X" pattern visible in the top panel of the data cube. This top panel is a time slice through one of the reflection events.

Kjartansson (1979) made plots of trace power in midpoint-offset coordinates and observed "V" shaped patterns due to shallow velocity or absorption anomalies in the Grand Isle data set (see also Claerbout (1993)). In Figure 4, I have plotted trace power for three different synthetic data sets with velocity anomalies centered

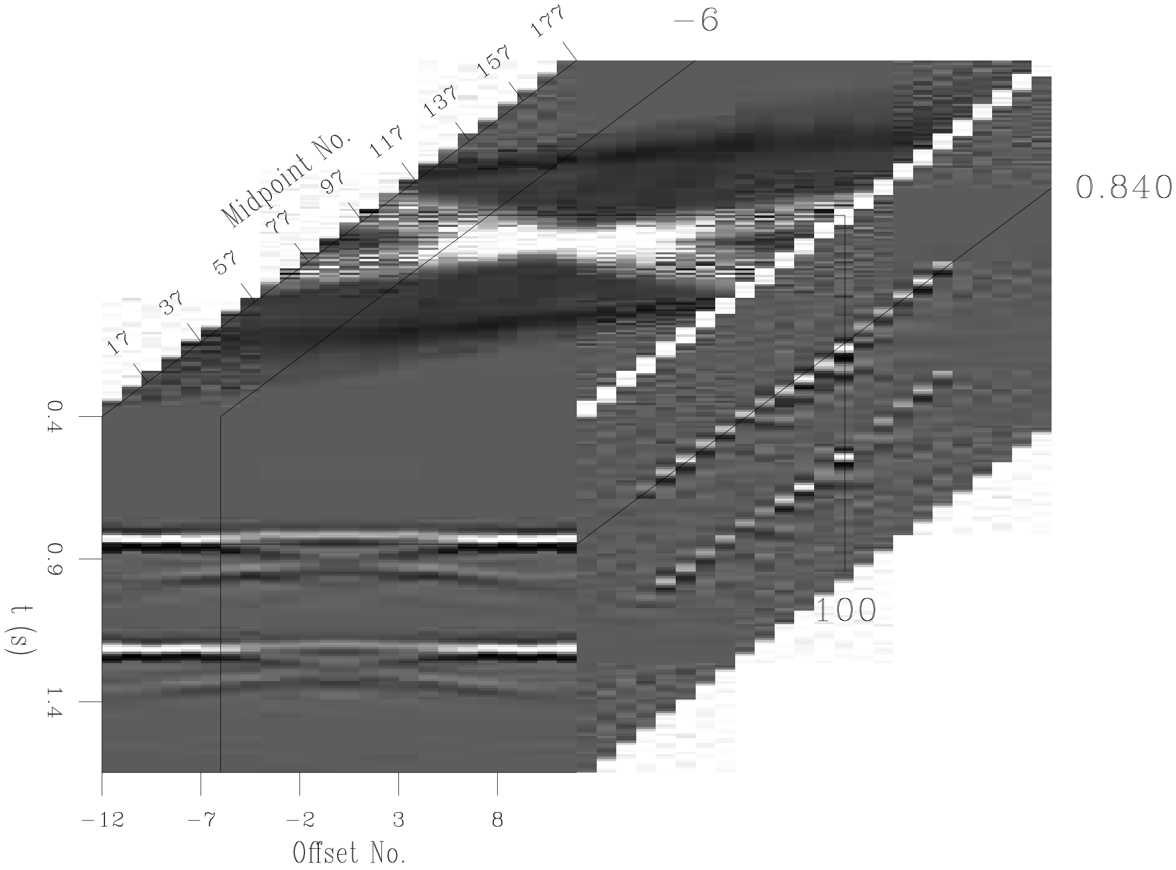

Figure 3: Synthetic CMP data after NMO correction. The velocity perturbation causes the distinctive “X” pattern visible in the time slice. dimitri-synupnmo [ER]

at depths of 0.1 km, 0.2 km and 0.3 km. The trace power is calculated by taking the square root of the sum of the squares of the trace amplitudes. The "X" patterns arise because the synthetics are split spread to simulate land data acquisition. For deeper anomalies the legs of the "X" are closer to the midpoint axis. For shallower anomalies the legs of the "X" are closer to the 45° lines representing the shot and group axes.

The qualitative observation that the trajectory of the "X" patterns is a function of anomaly depth gives rise to the slant stack imaging method of the next section.

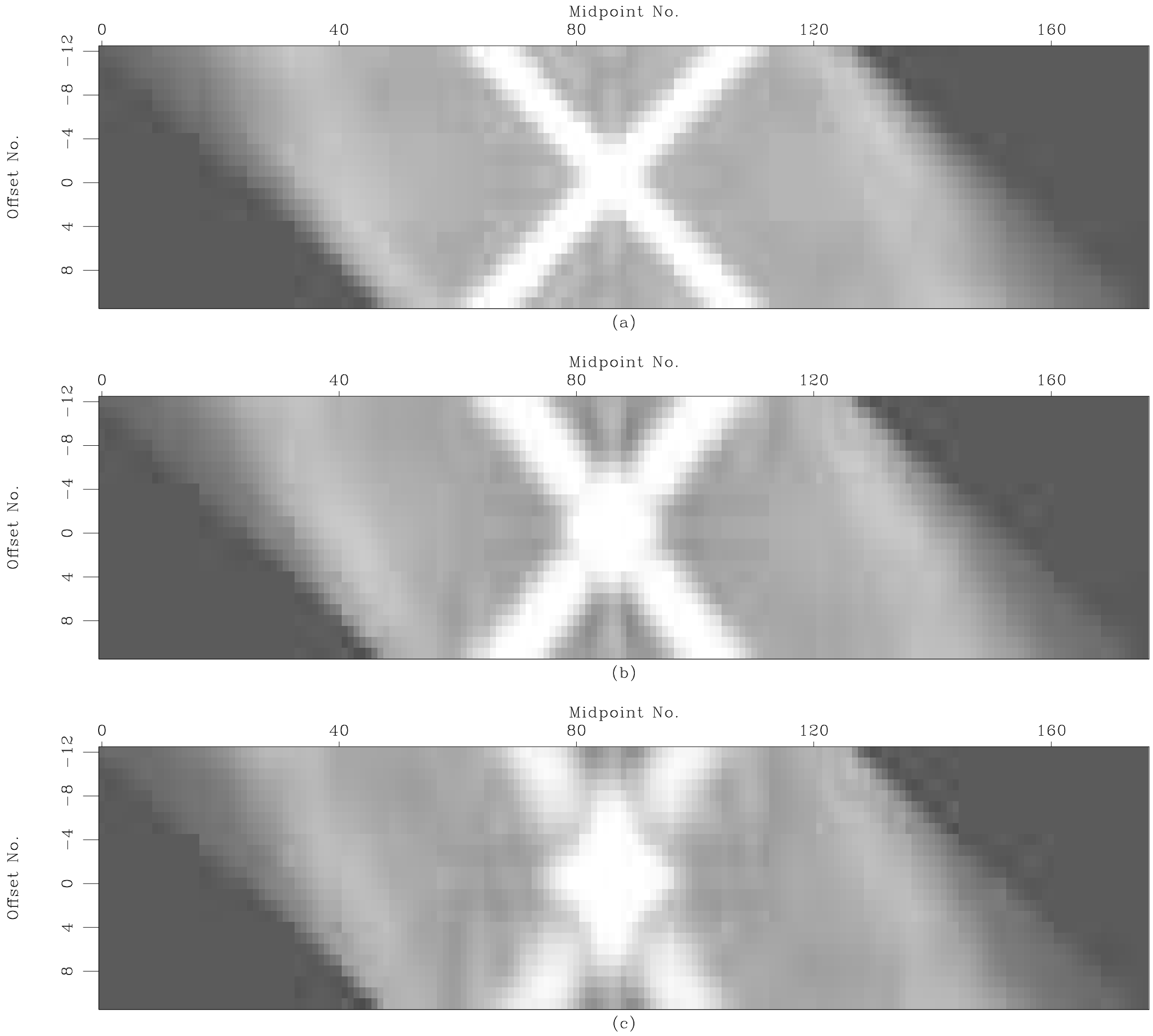

Figure 4: The trace power in midpoint-offset coordinates after NMO is displayed for velocity perturbations (a) at shallow depth, (b) at intermediate depth, and (c) at greater depth. The depth in (b) is the same as the depth in Figures 1 through 3. The shallower anomaly has energy closer to the shot and group axes. dimitri-power3 [ER]

ESTIMATION OF NEAR SURFACE VELOCITY

Kjartansson found that he could locate near surface anomalies but he did not provide a method of estimating velocity. In this section I propose a two-part method of estimating the velocity:

- Slant stack inversion of trace power data to locate the velocity anomalies in midpoint and depth.
- Iterative downward continuation of the data through the near surface model obtained in the first step to determine $v(x, z)$.

The method is not yet complete and both aspects of the problem still require work. In this section I will present how each part of the method works.

Slant stack imaging

Because the dip of the "X" patterns in Figure 4 can be interpreted as a measure of depth, it is possible to image near surface velocity perturbations by performing slant stacks of the power plots. I use a slightly modified version of the conjugate gradient slant stack inversion code written by Claerbout (1993) to locate the anomalies.

The input to the algorithm is the logarithm of the power plots shown in Figure 4. Ten steps of conjugate gradient are used to minimize

$$S\, m \;\approx\; d$$

where S is the inverse slant stack operator, d is the input power map, and m is the unknown velocity structure.

The results of the slant stack inversion are presented along with the power plots in Figure 5. In all cases the image of the anomaly occurs directly below the center of the "X". The images exhibit artifacts at the bottom of the plot which are probably due to data truncation. The reconstructed image shows the anomaly to be just below the surface. It is clear that as the depth of the anomaly increases, the image moves deeper.

Although the slant stack reconstruction qualitatively images the anomaly, more work is required to refine the algorithm, eliminate artifacts and increase resolution. The relationship between the pseudo-depth of the images and the actual depth has also not yet been worked out. Resolution is limited by the small input data set and by unresolved imperfections in the imaging algorithm.

Downward continuation

Ultimately, I would like to input an initial image from this slant stack result into a downward continuation program as a first guess at the velocity structure. This

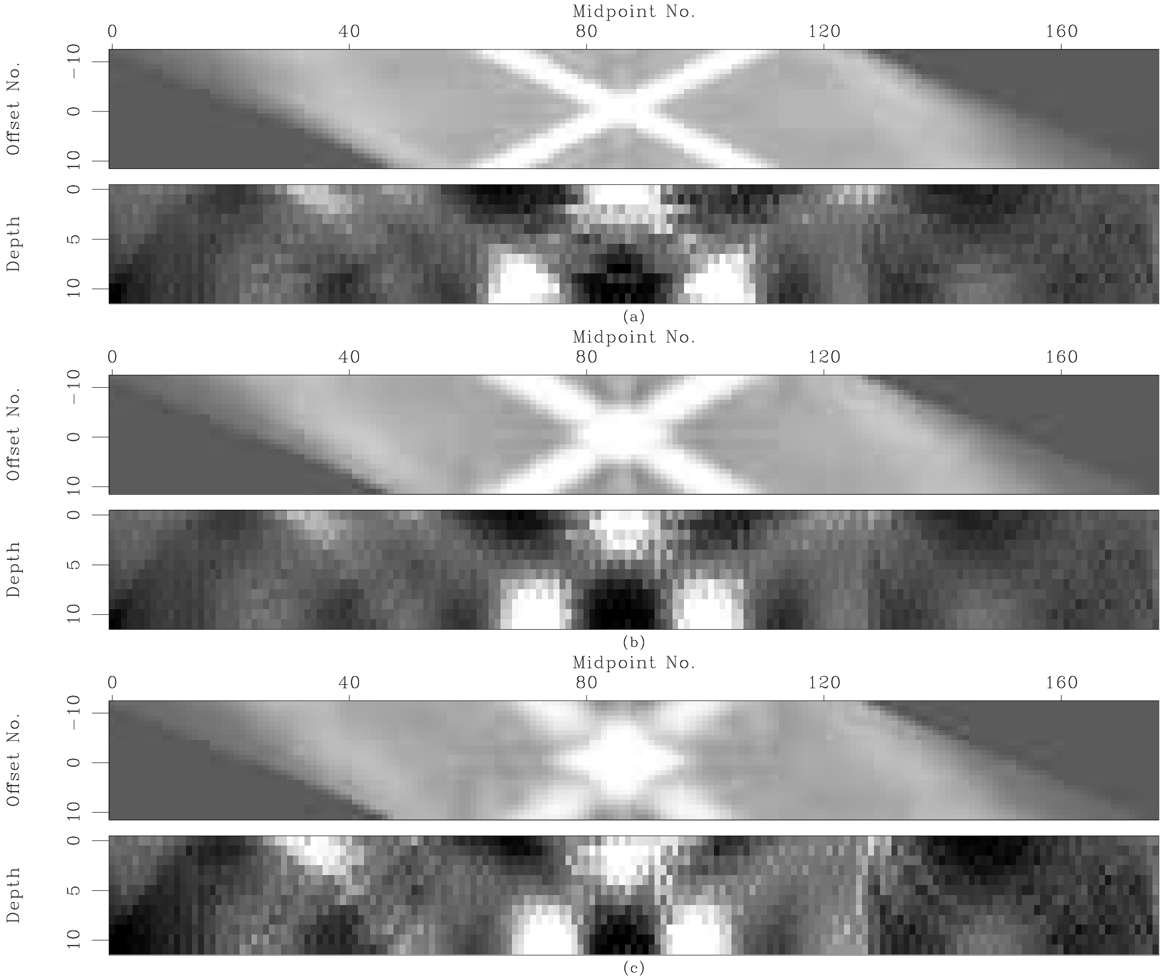

Figure 5: The trace power maps and depth images are displayed for velocity perturbations at three different depths. (a) The top two plots are for a velocity perturbation at shallow depth, (b) the middle two are for a velocity perturbation at intermediate depth, and (c) the bottom two are for a velocity perturbation at greater depth. The image of the velocity perturbation is the blob of energy directly below the surface in the center of the plots. As the anomaly gets deeper the legs of the "X" get closer together and the images move further away from the surface. $\boxed{\text{dimitri-tomoall}}$ [ER]

first guess could then be refined using an iterative method. The criteria for when a satisfactory velocity has been converged upon could then be the elimination of the "X" patterns and/or hyperbolic trajectories in shot or offset space. Both these criteria are essentially the same and will be satisfied when an adequate velocity is converged upon.

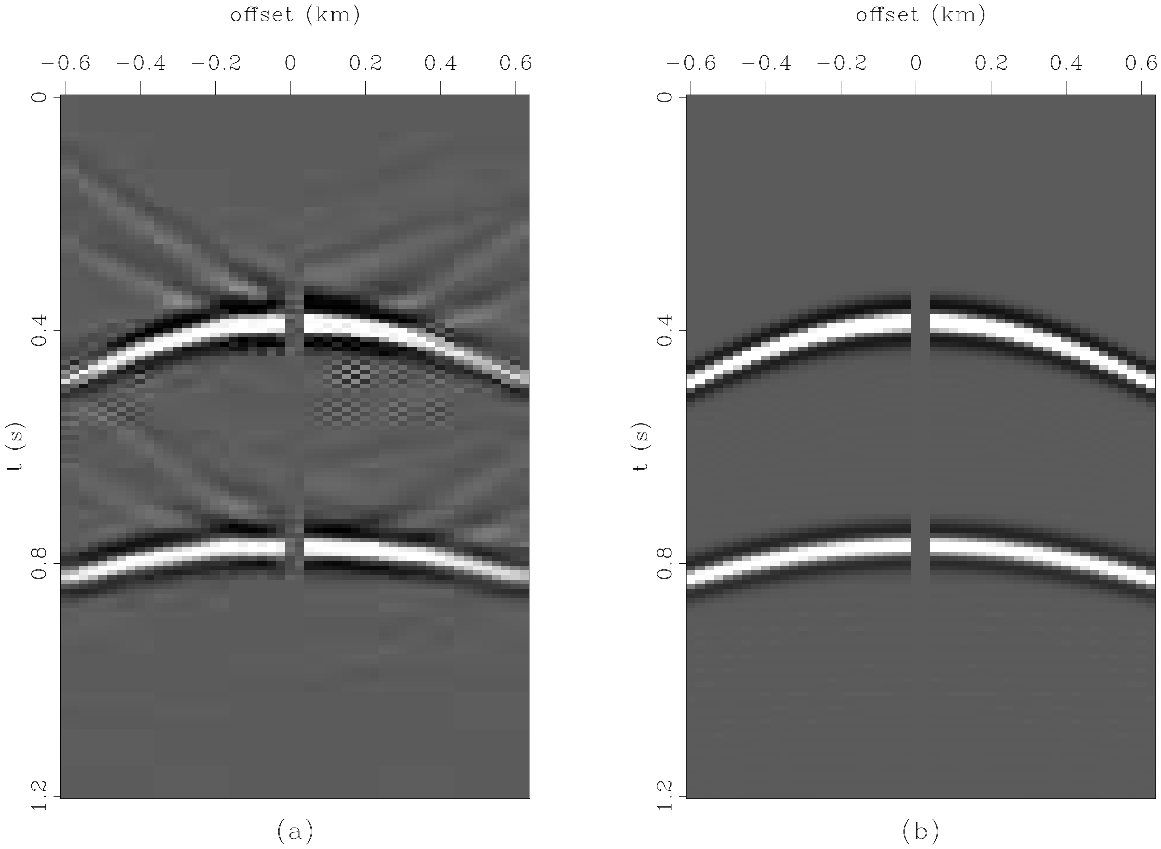

Figure 6: Comparison of (a) a synthetic shot gather downward continued through the velocity perturbation with the exact velocity model and (b) the original synthetic data. dimitri-syndn [ER]

At the time of this writing, I am not ready to input the result of the slant stack code into the downward continuation code; However, I can demonstrate how the distortions due to the velocity perturbation can be removed. In Figure 6a I have taken the data from Figures 2b and 3 and downward continued through the exact velocity model. The effect of the velocity perturbation is removed. The kinematics are restored but some artifacts and amplitude effects remain. This downward continuation is performed using the Kirchhoff code discussed earlier. In order to parameterize velocity it will be more convenient to perform the wavefield extrapolation by using a finite-difference code or by calculating finite-difference traveltimes for the Kirchhoff scheme.

CONCLUSIONS

The synthetic modeling results confirm the point that near surface velocity variations create not only timing anomalies, but also focusing anomalies. These focusing anomalies cannot be compensated for by static shift. Near surface variations cause distinct trajectories in midpoint-offset plots of trace power. Preliminary results show that slant stack imaging based on these power plots can be used to locate velocity perturbations. Once these perturbations are located, the seismic wavefield can be extrapolated through the near surface to iteratively estimate velocity. Much work remains to be done in order to implement and link these two steps, but the results presented here are encouraging.

REFERENCES

Bevc, D., and Claerbout, J., 1993, Choice of integration method for anti-aliased Kirchhoff migration: SEP–**77**, 295–302.

Bevc, D., 1993, Data parallel wave equation datuming: SEP–**77**, 131–140.

Claerbout, J. F., 1985, Imaging the Earth's Interior: Blackwell Scientific Publications.

Claerbout, J. F., 1993, Reflection tomography: Kjartansson revisited: SEP–**79**, 59–68.

Kjartansson, E., 1979, Attenuation of seismic waves in rocks and applications in energy exploration: SEP–**23**.